Article

Importance of Orbital Optimization for Double-Hybrid Density Functionals: Application of the OO-PBE-QIDH Model for Closed- and Open-Shell Systems

Juan Carlos Sancho-García, Ángel José Pérez-Jiménez,
Marika Savarese, Eric Bremond, and Carlo Adamo

1
2
3
4
5
6
7
8
9
10
11
12
13
14
15
16
17
18
19
20
21
22
23
24
25
26
27
28
29
30
31
32
33
34
35
36
37
38
39
40
41
42
43
44
45
46
47
48
49
50
51
52
53
54
55
56
57
58
59
60

Importance of Orbital Optimization for Double-Hybrid Density Functionals: Application of the OO-PBE-QIDH Model for Closed- and Open-shell Systems

J. C. Sancho-García[1]*, A. J. Pérez-Jiménez[1],
M. Savarese[2], E. Brémond[2], and C. Adamo[2,3,4]

[1] Departamento de Química Física,
Universidad de Alicante, 03080 Alicante, Spain

[2] CompuNet, Istituto Italiano di Tecnologia,
via Morego 30, I-16163 Genoa, Italy

[3] Institut de Recherche de Chimie Paris,
IRCP CNRS UMR-8247, Chimie ParisTech,
École Nationale Superieure de Chimie de Paris,
11 rue P. et M. Curie, F-75231 Paris Cedex 05, France

[4] Institut Universitaire de France,
103 Boulevard Saint Michel, F-75005 Paris, France

February 22, 2016

*E-mail: jc.sancho@ua.es

1

1
2
3
4
5
6
7
8
9
10
11
12
13
14
15
16
17
18
19
20
21
22
23
24
25
26
27
28
29
30
31
32
33
34
35
36
37
38
39
40
41
42
43
44
45
46
47
48
49
50
51
52
53
54
55
56
57
58
59
60

Abstract

We assess here the reliability of orbital optimization for modern double-hybrid density functionals such as the parameter-free PBE-QIDH model. We select for that purpose a set of closed- and open-shell strongly and weakly bound systems, including some standard and widely used datasets, to show that orbital optimization improves the results with respect to standard models, notably for electronically complicated systems, and through first-order properties obtained as derivatives of the energy.

Key words: double-hybrid density functionals, orbital optimization, open-shell molecules, polycyclic aromatic hydrocarbons.

2

1   Introduction

Orbital-Optimization (OO) has been recently applied to various orders of Møller-Plesset perturbation theory, especially at the second-order for both the conventional (MP2) and its spin-component scaled (SCS-MP2) version, revealing itself as a very powerful tool for dealing with open-shell systems or when spin contamination is a major issue.[1,2] In these cases, the zeroth-order Slater determinant may be a poor reference, and then the perturbative expansion becomes divergent and unreliable, while it has been shown that OO-MP2 repairs those poor zeroth-order orbitals and leads to better results for reaction barriers and properties involving free radicals.[3,4] On the other hand, MP2-like contribution is a natural ingredient of any Double-Hybrid (DH) density functional,[5–7] although in a weighted contribution to the total exchange-correlation according to each strategy followed during their development, therefore inheriting (partly) the advantages and pitfalls of MP2 theory too. Actually, Peverati and Head-Gordon[8] were the first to recognize (up to the best of our knowledge) the importance of this issue within the field of Density Functional Theory (DFT), applying consequently an orbital-optimization scheme to the PBE0-DH[9] and PBE0-2[10] double-hybrid models. Compared with the large improvement formerly obtained for the OO-MP2 method, they found a more modest impact on their results when going from DHs to OO-DHs, which was attributed to the fact that this contribution is weighted in the latter models by a factor always lower than unity.

However, the orbitals effects in DH functionals is gaining interest, with the performance of some functionals largely relying on the underlying orbitals used to feed all the energy terms entering into their formulation.[11–14] It seems thus timely to explore the possibilities of orbital-optimization for the last-

3

generation of double-hybrid functionals. Therefore, we extend pioneering studies to the PBE-QIDH form,[15] a parameter-free model developed under the framework of the adiabatic connection model, and perform an additional benchmark study aiming also to disclose some new results and insights on challenging applications to conjugated molecules.

2   Theoretical details

As it was said before, we select a recently developed (the PBE-QIDH exchange-correlation functional) model for several reasons: (i) it has been extensively benchmarked in last years and, despite being a parameter-free model, its accuracy becomes fully competitive with that of parameterized ones;[16,17] (ii) it has been shown to provide a rational framework for general-like hybridization schemes, independently of the underlying exchange-correlation form selected;[18] and (iii) it keeps a relevant contribution (*vide infra*) of the added perturbative correlation. The general form of this model is:

$$E_{xc} = \lambda_x E_x^{\text{EXX}}[\phi] + (1 - \lambda_x)E_x[\rho] + \lambda_c E_c^{\text{PT2}}[\phi, \phi'] + (1 - \lambda_c)E_c[\rho], \quad (1)$$

where $\lambda_x = 3^{-1/3}$ and $\lambda_c = \frac{1}{3}$, both values being rationally obtained without any parameterization, and $E_c^{\text{PT2}}[\phi, \phi']$ is the second-order perturbation theory contribution, for which the explicit dependence on both the set of occupied (ϕ) and virtual (ϕ') orbitals is underlined. This set of orbitals is normally obtained by iteratively solving the Kohn-Sham (KS) equations and then using the manifold of orbitals to feed (*a posteriori* and thus without further self-consistency) the E_c^{PT2} contribution. The above minimization is necessarily done in an approximate way, since exactly solving for an orbital-dependent functional would need to invoke the Optimized Effective Potential

4

(OEP) method.[19–22]

Therefore, contrarily to the standard and widely used approach, we also self-consistently minimize here the perturbation energy with respect to the amplitudes and the total energy with respect to changes in orbitals,[3] and thus obtaining orbitals adapted to the perturbative field, leading to a fully variational perturbation energy that is finally scaled by λ_c and added to the previous DFT-based energy contributions.[8] In other words, we now independently calculate both the orbitals entering into the first three terms of Eq. (1) and those for the E_c^{PT2} contribution. Results obtained with this method will be coined as OO-PBE-QIDH in the following. Note that the computational cost of the latter method is neccesarily higher than that for PBE-QIDH, since every iteration of the OO-based procedure is as costly as an MP2 calculation, and that some divergences may also occur, but are normally cured by choosing an appropriate level shift parameter.[23]

All the calculations reported here were done with the ORCA package[24] (release 3.0.1) using the following criteria: (i) the family of (aug-)cc-pVnZ basis sets[25] was used, with n their cardinal number, together with the corresponding auxiliary basis sets (aug-)cc-pVnZ/C when the 'resolution-of-the-identity' (RI) technique was exploited for the (more costly) E_c^{PT2} term;[26] (ii) we increased systematically the numerical thresholds for the SCF calculations (i.e., keywords TightSCF, Grid6, NoFinalGrid); (iii) we correlated all electrons (i.e., keyword NoFrozenCore) for calculating the perturbation correction; and (iv) spin-unrestricted methods were used for all open-shell systems.

5

3 Results and discussion

3.1 Application to standard databases

We apply first both PBE-QIDH and OO-PBE-QIDH methods to some datasets of large interest, as originally developed,[27,28] such as the AE6 (atomization energies of small molecules), IP13 (ionization potentials of small molecules) and SIE11 (reactions prone to self-interaction errors), with the very large aug-cc-pVQZ basis set to avoid any basis set incompleteness issue. We choose as metrics to evaluate the performance of the methods the Mean Deviation (MD), Mean Absolute Deviation (MAD) and Root Mean-Squared Deviation (RMSD) with respect to reference results, presenting the results in Table 1. The overall inspection shows very slight improvement and/or deterioration of results when using OO-PBE-QIDH instead of PBE-QIDH. The results provided by both methods are in the range of accuracy expected for the family of double-hybrid functionals. For instance, the PBE0-DH and PBE0-2 models yield MAD values of 2.75 and 1.89 kcal/mol, respectively, for the IP13 database.[8] Taking now the SIE11 dataset as example, OO-PBE-QIDH gives a RMSD of 4.75 kcal/mol, compared with the values provided by the B2-PLYP,[29] PWPB95,[27] or XYG3[30] models, which are 6.10, 4.96, and 3.94 kcal/mol, respectively.[27]

We tackle now the reaction energies for some Diels-Alder reaction cycloadditions (the dataset dubbed DARC4 in Table 1), whose reactants and products are displayed in Figure 1. These reactions have respectively butadiene and ethene (DARC-1), butadiene and ethyne (DARC-2), cyclopentadiene and ethene (DARC-3), cyclopentadiene and ethyne (DARC-4), as reactants, giving the condensed products specified in all cases. These reactions are also part of the large GMTKN30 database,[27] and are known to be challenging

6

to modern semilocal density functionals.[31] The results of PBE-QIDH and OO-PBE-QIDH calculations are gathered in Table 2, finding again similar results for both methods and in line with those obtained using other sophisticated methods,[32] although however more accurate results (MAD of 5.01 and RMSD of 5.31 kcal/mol) are found when employing parameterized double-hybrid methods like B2-PLYP.

Furthermore, we have also included a representative dataset for forward and backward heavy-atom transfer reactions, namely HATBH12,[33] which is part of the larger DBH24 database[34] and includes the BH6 pioneering dataset[35] together with additional reactions. As can be seen from Table 1, the MAD and RMSD values are roughly halved for OO-PBE-QIDH (2.96 and 2.92 kcal/mol) with respect to the PBE-QIDH (4.82 and 4.84 kcal/mol) model. We attribute the larger accuracy of the OO-PBE-QIDH model, which becomes competitive with other highly accurate *ab initio* methods like QCISD(T) or density functionals specifically parameterized for kinetics,[33] to the good description of all kind of species (i.e., neutral or free radicals) involved in the reactions either as reactants, products or transition states.

3.2　Potential energy curves of the O_2^+ radical cation

The ground-state ($^2\Pi$) dissociation of the O_2^+ radical cation is a prototypical case for studying spatial symmetry-breaking, which is known to be especially difficult for theoretical methods. The use of a symmetry-broken Unrestricted Hartree-Fock (UHF) solution as starting point for perturbative methods (e.g. Møller-Plesset theory) is known to be largely affected by: (i) a poor behaviour of perturbative expansions at intermediate and large

7

interatomic distances;[36] (ii) spin-contamination issues;[37] and (iii) a lack of convergence for higher orders of perturbation theory.[38] On the other hand, spin-projection for DFT calculations is not recommended neither[39] and more involved approaches (i.e. multiconfigurational) are thus needed,[40–42] which necessarily goes beyond the scope of this study. However, orbital-optimized double-hybrid methods might constitute an alternative approach for dealing with open-shell molecules at all distances, and we will thus explore here the performance of (standard) PBE-QIDH and (novel) OO-PBE-QIDH methods for this challenging case.

Figure 2 displays the potential energy curve upon bond stretching, as well as how the dipole moment evolves along bond dissociation. We can easily see for PBE-QIDH, as well as for other double-hybrid models recently applied in the literature,[8] that the spatial symmetry is broken at around 1.9 Å, featuring concomitantly a discontinuity in those first-order properties (e.g. dipole moment) computed, similarly to the MP2 case, although once again necessarily attenuated by the weight of the λ_c parameter entering into the formulation of the former methods.[43] Interestingly, the OO-PBE-QIDH method shows continuous results, for both zero- and first-order properties, at all intermediate and large distances. The latter method also slightly improves the equilibrium distance (1.106 Å) and harmonic vibrational frequency (1988 cm^{-1}) with respect to the PBE-QIDH results of 1.104 Å and 2017 cm^{-1}, to be compared with experimental values of 1.116 Å and 1905 cm^{-1}. In other words, it seems that properties near the equilibrium region are not degraded with orbital-optimization while they improve at larger internuclear distances.

8

3.3   Weakly bound open-shell systems

Interactions of radicals with water molecules are particularly interesting, not only by their relevance in aquatic or atmospheric chemistry, but also by the type of the chemical bonding ("hemi-" or "two-center-three-electron" bonds) formed.[44] We study here the set of $H_2O \cdots F$, $H_2O \cdots Cl$, $H_2O \cdots Br$, $H_2O \cdots Li$, $H_2O \cdots Al$, and $H_2O \cdots Be^+$ weakly bound complexes (see Figure 3a) at the CCSD(T)/aug-cc-pVTZ optimized geometries taken from Ref.[45] The results shown in Table 3 reveal again a good and robust performance of both the PBE-QIDH and OO-PBE-QIDH methods, with values of MAD or RMSD slightly below and above, respectively, of the "chemical accuracy" threshold of $\pm$ 1 kcal/mol. Note that these low values are very competitive compared with those provided by B2-PLYP (MAD of 0.89 kcal/mol) or XYG3 (MAD of 0.98 kcal/mol) models,[45] as well as with respect to other (more costly) *ab initio* methods like MP3 or CCSD,[46] and that the inclusion of a dispersion correction did not affect the results (MAD of 1.09 kcal/mol now for B2-PLYP-D) in the right direction.

We finally tackle the non-ionic (C_{6v}) Li-C_6H_6 weakly bound complex (see also Figure 3b) which has been thoroughly studied as a model for more complex Li-graphene interactions[47] or to disentangle how the different electronic structure methods can give the correct energy order between the competing ionic (C_{2v}) and non-ionic models for this interaction.[48] Figure 4 displays the dissociation curve, for which we can estimate an equilibrium distance of $d = 2.11$ Å and an energy well of $\Delta E = -6.00$ kcal/mol at the PBE-QIDH level, noting that the OO-PBE-QIDH only slightly alter these values ($d = 2.12$ Å and $\Delta E = -5.93$ kcal/mol), to be favourably compared with previous estimates at the SCS-MP2/aug-cc-pVTZ level ($d = 2.29$ Å and

9

$\Delta E = -5.66$ kcal/mol).[49] Interestingly, the Lödwin or Mülliken spin population on the Li atom, which should remain nearly constant and close to unity for a purely non-ionic complex, significantly deviates with the PBE-QIDH model (see Figure 4), with orbital optimization recovering a smoother behaviour at all distances in fully agreement with modern orbital-optimized opposite-spin MP2-based methods.[50]

3.4   Linear and cyclic (oligo)acenes

Subtle electronic effects dominate the singlet-triplet energy gap of polyciclic aromatic hydrocarbons such as (oligo)acenes.[51] If their ground-state is a closed-shell singlet or an open-shell triplet has been a question of recent studies,[52,53] with some DFT results predicting (wrongly) a cross over and thus a ferromagnetic (triplet) state as the most stable one. On the other hand, the projection to pure spin states,[54] or carefully performed *ab initio* calculations,[55] has helped to bracket previous DFT efforts, thus confirming a singlet ground-state for short and long (oligo)acenes.[56,57] We present in Table 4 the results of our calculations for the adiabatic singlet-triplet energy gap of fused benzene rings, from benzene to hexacene, and compare them with experimental values normally obtained in inert matrices.[58] The singlet state is always favoured when the PBE-QIDH method is applied, resulting in a positive value for the singlet-triplet gap for all chain lengths, in both qualitative and quantitative agreement with previous results at the B2-PLYP-D/TZVP level (MAD = 4.43 kcal/mol).[59] We emphasize the greater accuracy of the OO-PBE-QIDH method, for which a MAD = 2.58 kcal/mol is obtained, especially for the longest systems considered here. Actually, the evolution of the values as a function of the fused benzene rings is graphically

10

shown in Figure 5, where the corresponding experimental values, as well as their error bar for pentacene and hexacene, are also included. We can see how the PBE-QIDH and OO-PBE-QIDH results start to significantly differ from anthracene onwards, with the latter practically superimposing the experimental values for tetracene, pentacene, and hexacene (differences lower than 0.03 eV).

Turning now the attention to the cyclic form of (oligo)acenes,[60] we note first that: (i) due to their highly strained form (see Figure 6) only the longest oligomers can be envisioned as synthetic targets; and (ii) for closely related systems, $[5.5.6]_n$cyclacenes, recent investigations questioned the accuracy of B2-PLYP-D3, with respect to more modern double-hybrid forms (PWRB95) based on the random phase approximation, and attributed this behaviour to the PT2 part.[61] We thus calculate for the 6-cyclacene molecule (the analogue of the hexacene) an adiabatic singlet-triplet value of 10.74 and 6.76 kcal/mol at the PBE-QIDH and OO-PBE-QIDH levels, respectively. This positive value predicts a triplet state higher in energy than a closed-shell ground-state, contrarily to a negative value predicted by standard DFT calculations.[62] However, the OO-PBE-QIDH calculated singlet-triplet energy gap is roughly halved with respect to that of the parent linear compound, which can anticipate a different evolution of triplet energies with system size than that obtained for the linear forms.

4   Conclusions

Here we have analyzed the influence of optimizing the orbitals entering into the perturbative contribution of the parameter-free PBE-QIDH double-

11

hybrid functional. These OO-PBE-QIDH results suggest a negligible impact on the energetics of ground-state systems near their equilibrium geometry. However, it becomes of primary importance whenever a substantial change in the orbitals is needed to capture the essential physics of the problem, and then obtaining accurate estimates of properties beyond the equilibrium region or for excited-states. We have concomitantly cross-validated the accuracy of the original PBE-QIDH model, resulting fully competitive with other double-hybrid expressions. The above guidelines might be helpful to select an appropriate methodology for electronically difficult systems and rare scenarios, for which orbital-optimized approaches might be certainly useful.

Acknowledgements

References

[1] Lochan, R. C.; Head-Gordon, M. Orbital-optimized opposite-spin scaled second-order correlation: An economical method to improve the description of open-shell molecules. *The Journal of chemical physics* **2007**, *126*, 164101.

[2] Kossmann, S.; Neese, F. Efficient structure optimization with second-order many-body perturbation theory: The RIJCOSX-MP2 method. *Journal of chemical theory and computation* **2010**, *6*, 2325–2338.

[3] Neese, F.; Schwabe, T.; Kossmann, S.; Schirmer, B.; Grimme, S. Assess-

12

ment of orbital-optimized, spin-component scaled second-order many-body perturbation theory for thermochemistry and kinetics. *Journal of chemical theory and computation* **2009**, *5*, 3060–3073.

[4] Bozkaya, U. Orbital-Optimized MP3 and MP2.5 with Density-Fitting and Cholesky Decomposition Approximations. *Journal of Chemical Theory and Computation* **2016**,

[5] Zhang, I. Y.; Xu, X. Doubly hybrid density functional for accurate description of thermochemistry, thermochemical kinetics and nonbonded interactions. *International Reviews in Physical Chemistry* **2011**, *30*, 115–160.

[6] Sancho-García, J. C.; Adamo, C. Double-hybrid density functionals: merging wavefunction and density approaches to get the best of both worlds. *Physical Chemistry Chemical Physics* **2013**, *15*, 14581–14594.

[7] Goerigk, L.; Grimme, S. Double-hybrid density functionals. *Wiley Interdisciplinary Reviews: Computational Molecular Science* **2014**, *4*, 576–600.

[8] Peverati, R.; Head-Gordon, M. Orbital optimized double-hybrid density functionals. *The Journal of chemical physics* **2013**, *139*, 024110.

[9] Brémond, E.; Adamo, C. Seeking for parameter-free double-hybrid functionals: the PBE0-DH model. *The Journal of chemical physics* **2011**, *135*, 024106.

[10] Chai, J.-D.; Mao, S.-P. Seeking for reliable double-hybrid density functionals without fitting parameters: The PBE0-2 functional. *Chemical Physics Letters* **2012**, *538*, 121–125.

13

[11] Zhang, I. Y.; Su, N. Q.; Brémond, É. A.; Adamo, C.; Xu, X. Doubly hybrid density functional xDH-PBE0 from a parameter-free global hybrid model PBE0. *The Journal of chemical physics* **2012**, *136*, 174103.

[12] Kesharwani, M. K.; Kozuch, S.; Martin, J. M. Comment on "Doubly hybrid density functional xDH-PBE0 from a parameter-free global hybrid model PBE0" [J. Chem. Phys. 136, 174103 (2012)]. *The Journal of chemical physics* **2015**, *143*, 187101.

[13] Zhang, I. Y.; Su, N. Q.; Brémond, É. A.; Adamo, C.; Xu, X. Response to "Comment on Doubly hybrid density functional xDH-PBE0 from a parameter-free global hybrid model PBE0" [J. Chem. Phys. 143, 187101 (2015)]. *Journal of Chemical Physics* **2015**, *143*, 7102.

[14] Su, N. Q.; Xu, X. A comparative study of the xDH-PBE0 and DSD-PBEPBE-D3BJ doubly hybrid density functionals. *Molecular Physics* **2015**, 1–11.

[15] Brémond, É.; Sancho-García, J. C.; Pérez-Jiménez, Á. J.; Adamo, C. Communication: Double-hybrid functionals from adiabatic-connection: The QIDH model. *The Journal of chemical physics* **2014**, *141*, 031101.

[16] Wykes, M.; Su, N. Q.; Xu, X.; Adamo, C.; Sancho-García, J.-C. Double Hybrid Functionals and the Π-System Bond Length Alternation Challenge: Rivaling Accuracy of Post-HF Methods. *Journal of Chemical Theory and Computation* **2015**, *11*, 832–838.

[17] Wykes, M.; Pérez-Jiménez, A.; Adamo, C.; Sancho-García, J. The diene isomerization energies dataset: A difficult test for double-hybrid density functionals? *The Journal of chemical physics* **2015**, *142*, 224105.

14

[18] Brémond, É.; Savarese, M.; Pérez-Jiménez, Á. J.; Sancho-García, J. C.; Adamo, C. Systematic Improvement of Density Functionals through Parameter-Free Hybridization Schemes. *The journal of physical chemistry letters* **2015**, *6*, 3540–3545.

[19] Engel, E.; Vosko, S. Accurate optimized-potential-model solutions for spherical spin-polarized atoms: Evidence for limitations of the exchange-only local spin-density and generalized-gradient approximations. *Physical Review A* **1993**, *47*, 2800.

[20] Grabo, T.; Gross, E. K. Density-functional theory using an optimized exchange-correlation potential. *Chemical physics letters* **1995**, *240*, 141–150.

[21] Hirata, S.; Ivanov, S.; Grabowski, I.; Bartlett, R. J.; Burke, K.; Talman, J. D. Can optimized effective potentials be determined uniquely? *The Journal of Chemical Physics* **2001**, *115*, 1635–1649.

[22] Kümmel, S.; Perdew, J. P. Optimized effective potential made simple: Orbital functionals, orbital shifts, and the exact Kohn-Sham exchange potential. *Physical Review B* **2003**, *68*, 035103.

[23] Stück, D.; Head-Gordon, M. Regularized orbital-optimized second-order perturbation theory. *The Journal of chemical physics* **2013**, *139*, 244109.

[24] Neese, F. The ORCA program system. *Wiley Interdisciplinary Reviews: Computational Molecular Science* **2012**, *2*, 73–78.

[25] Dunning Jr, T.; Peterson, K.; Woon, D. Correlation consistent basis sets for molecular calculations. *Encyclopedia of Computational Chemistry* **1998**, 88–115.

15

[26] Neese, F. An improvement of the resolution of the identity approximation for the formation of the Coulomb matrix. *Journal of computational chemistry* **2003**, *24*, 1740–1747.

[27] Goerigk, L.; Grimme, S. Efficient and Accurate Double-Hybrid-Meta-GGA Density Functionals Evaluation with the Extended GMTKN30 Database for General Main Group Thermochemistry, Kinetics, and Noncovalent Interactions. *Journal of chemical theory and computation* **2010**, *7*, 291–309.

[28] Haoyu, S. Y.; Zhang, W.; Verma, P.; He, X.; Truhlar, D. G. Nonseparable exchange–correlation functional for molecules, including homogeneous catalysis involving transition metals. *Physical Chemistry Chemical Physics* **2015**, *17*, 12146–12160.

[29] Grimme, S. Semiempirical hybrid density functional with perturbative second-order correlation. *The Journal of chemical physics* **2006**, *124*, 034108.

[30] Zhang, Y.; Xu, X.; Goddard, W. A. Doubly hybrid density functional for accurate descriptions of nonbond interactions, thermochemistry, and thermochemical kinetics. *Proceedings of the National Academy of Sciences* **2009**, *106*, 4963–4968.

[31] Tognetti, V.; Cortona, P.; Adamo, C. Activation enthalpies of pericyclic reactions: the performances of some recently proposed functionals. *Theoretical Chemistry Accounts* **2009**, *122*, 257–264.

[32] Ruzsinszky, A.; Zhang, I. Y.; Scheffler, M. Insight into organic reactions from the direct random phase approximation and its corrections. *The Journal of chemical physics* **2015**, *143*, 144115.

16

[33] Zhao, Y.; González-García, N.; Truhlar, D. G. Benchmark database of barrier heights for heavy atom transfer, nucleophilic substitution, association, and unimolecular reactions and its use to test theoretical methods. *The Journal of Physical Chemistry A* **2005**, *109*, 2012–2018.

[34] Zheng, J.; Zhao, Y.; Truhlar, D. G. Representative benchmark suites for barrier heights of diverse reaction types and assessment of electronic structure methods for thermochemical kinetics. *Journal of chemical theory and computation* **2007**, *3*, 569–582.

[35] Lynch, B. J.; Truhlar, D. G. Small representative benchmarks for thermochemical calculations. *The Journal of Physical Chemistry A* **2003**, *107*, 8996–8999.

[36] Lepetit, M.; Pélissier, M.; Malrieu, J. Origins of the poor convergence of many-body perturbation theory expansions from unrestricted Hartree–Fock zeroth-order descriptions. *The Journal of chemical physics* **1988**, *89*, 998–1008.

[37] Wang, J.; Becke, A. D.; Smith Jr, V. H. Evaluation of $\langle \hat{S}^2 \rangle$ in restricted, unrestricted Hartree–Fock, and density functional based theories. *The Journal of chemical physics* **1995**, *102*, 3477–3480.

[38] Dunning Jr, T. H.; Peterson, K. A. Use of Møller–Plesset perturbation theory in molecular calculations: Spectroscopic constants of first row diatomic molecules. *The Journal of chemical physics* **1998**, *108*, 4761–4771.

[39] Wittbrodt, J. M.; Schlegel, H. B. Some reasons not to use spin projected density functional theory. *The Journal of chemical physics* **1996**, *105*, 6574–6577.

17

[40] Sancho-García, J.; Moscardó, F. Usefulness of the Colle–Salvetti model for the treatment of the nondynamic correlation. *The Journal of chemical physics* **2003**, *118*, 1054–1058.

[41] Garza, A. J.; Jiménez-Hoyos, C. A.; Scuseria, G. E. Capturing static and dynamic correlations by a combination of projected Hartree-Fock and density functional theories. *The Journal of chemical physics* **2013**, *138*, 134102.

[42] Garza, A. J.; Jiménez-Hoyos, C. A.; Scuseria, G. E. Electronic correlation without double counting via a combination of spin projected Hartree-Fock and density functional theories. *The Journal of chemical physics* **2014**, *140*, 244102.

[43] Kurlancheek, W.; Head-Gordon, M. Violations of N-representability from spin-unrestricted orbitals in Møller–Plesset perturbation theory and related double-hybrid density functional theory. *Molecular Physics* **2009**, *107*, 1223–1232.

[44] Gill, P. M.; Radom, L. Structures and stabilities of singly charged three-electron hemibonded systems and their hydrogen-bonded isomers. *Journal of the American Chemical Society* **1988**, *110*, 4931–4941.

[45] Tentscher, P. R.; Arey, J. S. Binding in radical-solvent binary complexes: benchmark energies and performance of approximate methods. *Journal of chemical theory and computation* **2013**, *9*, 1568–1579.

[46] Soydas, E.; Bozkaya, U. Accurate Open-Shell Noncovalent Interaction Energies from the Orbital-Optimized Møller–Plesset Perturbation Theory: Achieving CCSD Quality at the MP2 Level by Orbital Optimization. *Journal of Chemical Theory and Computation* **2013**, *9*, 4679–4683.

18

[47] Sadlej-Sosnowska, N. Ab Initio Study of Charge Transfer between Lithium and Aromatic Hydrocarbons. Can the Results Be Directly Transferred to the Lithium–Graphene Interaction? *The Journal of Physical Chemistry A* **2014**, *118*, 7044–7051.

[48] Denis, P. A.; Iribarne, F. C_{2V} or C_{6V}: Which is the most stable structure of the benzene–lithium complex? *Chemical Physics Letters* **2013**, *573*, 15–18.

[49] Vollmer, J. M.; Kandalam, A. K.; Curtiss, L. A. Lithium-benzene sandwich compounds: A quantum chemical study. *The Journal of Physical Chemistry A* **2002**, *106*, 9533–9537.

[50] Baker, T. A.; Head-Gordon, M. Modeling the charge transfer between alkali metals and polycyclic aromatic hydrocarbons using electronic structure methods. *The Journal of Physical Chemistry A* **2010**, *114*, 10326–10333.

[51] Rivero, P.; Jimenez-Hoyos, C. A.; Scuseria, G. E. Predicting Singlet–Triplet Energy Splittings with Projected Hartree–Fock Methods. *The Journal of Physical Chemistry A* **2013**, *117*, 8073–8080.

[52] Hachmann, J.; Dorando, J. J.; Avilés, M.; Chan, G. K.-L. The radical character of the acenes: A density matrix renormalization group study. *The Journal of chemical physics* **2007**, *127*, 134309.

[53] Jiang, D.-e.; Dai, S. Electronic ground state of higher acenes. *The Journal of Physical Chemistry A* **2008**, *112*, 332–335.

[54] San-Fabián, E.; Moscardó, F. On the actual nature of the antiferromagnetism shown by unrestricted calculations on conjugated hydrocarbon rings. *The European Physical Journal D* **2011**, *64*, 239–248.

19

[55] Hajgató, B.; Szieberth, D.; Geerlings, P.; De Proft, F.; Deleuze, M. A benchmark theoretical study of the electronic ground state and of the singlet-triplet split of benzene and linear acenes. *The Journal of chemical physics* **2009**, *131*, 224321.

[56] Casanova, D.; Head-Gordon, M. Restricted active space spin-flip configuration interaction approach: theory, implementation and examples. *Physical Chemistry Chemical Physics* **2009**, *11*, 9779–9790.

[57] Hajgató, B.; Huzak, M.; Deleuze, M. S. Focal point analysis of the singlet–triplet energy gap of octacene and larger acenes. *The Journal of Physical Chemistry A* **2011**, *115*, 9282–9293.

[58] Siebrand, W. Radiationless Transitions in Polyatomic Molecules. II. Triplet-Ground-State Transitions in Aromatic Hydrocarbons. *The Journal of Chemical Physics* **1967**, *47*, 2411–2422.

[59] Rayne, S.; Forest, K. A comparison of density functional theory (DFT) methods for estimating the singlet–triplet $(S_0 - T_1)$ excitation energies of benzene and polyacenes. *Computational and Theoretical Chemistry* **2011**, *976*, 105–112.

[60] Sadowsky, D.; McNeill, K.; Cramer, C. J. Electronic structures of [n]-cyclacenes (n= 6–12) and short, hydrogen-capped, carbon nanotubes. *Faraday Discussions* **2010**, *145*, 507–521.

[61] Grimme, S.; Steinmetz, M. A computationally efficient double hybrid density functional based on the random phase approximation. *Physical Chemistry Chemical Physics* **2016**,

20

[62] Choi, H. S.; Kim, K. S. Structures, magnetic properties, and aromaticity of cyclacenes. *Angewandte Chemie International Edition* **1999**, *38*, 2256–2258.

21

- **Table 1.** Statistics (kcal/mol) for the AE6, IP13, SIE11, DARC4, and HATBH12 datasets employed along this work, as calculated with the aug-cc-pVQZ basis set.

- **Table 2.** Interaction energies (kcal/mol) for $H_2O \cdots X$ open-shell weakly bound complexes, as calculated with the aug-cc-pVQZ basis set.

- **Table 3.** Adiabatic singlet-triplet energy gap (kcal/mol) for (oligo)acene molecules, as calculated with the cc-pVTZ basis set.

22

Table 1:

		PBE-QIDH	OO-PBE-QIDH
AE6	MD	-1.45	1.31
	MAD	4.80	4.96
	RMSD	5.66	6.38
IP13	MD	1.95	1.97
	MAD	2.09	2.11
	RMSD	2.74	2.75
SIE11	MD	3.45	3.89
	MAD	3.54	3.94
	RMSD	5.05	4.75
DARC4	MD	-9.12	-9.14
	MAD	9.12	9.14
	RMSD	9.28	9.29
HATBH12	MD	3.78	0.18
	MAD	4.82	2.96
	RMSD	4.84	2.92

23

Table 2:

Complex	PBE-QIDH	OO-PBE-QIDH	Reference[a]
$H_2O \cdots F$	-2.58	-3.89	-3.83
$H_2O \cdots Cl$	-3.75	-4.05	-3.69
$H_2O \cdots Br$	-3.76	-4.00	-3.52
$H_2O \cdots Li$	-12.96	-13.04	-12.39
$H_2O \cdots Al$	-9.82	-10.08	-7.59
$H_2O \cdots Be^+$	-65.59	-65.57	-64.20
MD	-0.54	-0.90	
MAD	0.96	0.90	
RMSD	1.22	1.22	

[a] Values calculated at the CCSD(T)/CBS level (taken from Ref.[45])

Table 3:

Reaction	PBE-QIDH	OO-PBE-QIDH	Reference[a]
benzene	93.95	92.32	84.34
naphtalene	67.89	66.16	60.90
anthracene	45.73	44.60	42.60
tetracene	32.18	30.07	29.45
pentacene	22.12	19.69	19.83 ± 0.70
hexacene	15.21	12.21	12.43 ± 1.20
MD	4.59	2.58	
MAD	4.59	2.58	
RMSD	5.26	4.00	

[a] Experimental values (taken from Ref.[55])

- **Figure 1.** Selected Diels-Alder condensation reactions (from top to bottom): butadiene + ethene → P1, butadiene + ethyne → P2, cyclopentadiene + ethene → P3, cyclopentadiene + ethyne → P4.

- **Figure 2.** Dissociation curves (top) and associated dipole moment (bottom) for the O_2^+ radical cation, as calculated with the cc-pVTZ basis set.

- **Figure 3.** Structures of the: (a) open-shell weakly bound $H_2O \cdots$ X, and (b) $C_6H_6 \cdots$ Li complexes. The distance between Li and the center of the benzene ring is 2.284 Å; X is a F, Cl, Br, Li, Al, or Be^+ atom at distances of 2.118, 2.604, 2.705, 1.888, 2.216, and 1.547 Å, respectively.

- **Figure 4.** Dissociation curves (top) and associated spin population on the Li atom (bottom) for the $C_6H_6 \cdots$ Li system, as calculated with the aug-cc-pVQZ basis set.

- **Figure 5.** Evolution of the adiabatic singlet-triplet energy gap of (oligo)acenes.

- **Figure 6.** Structures of the linear and cyclic ([6]cyclacene) forms of the hexacene molecule.

26

REACTANTS   PRODUCT

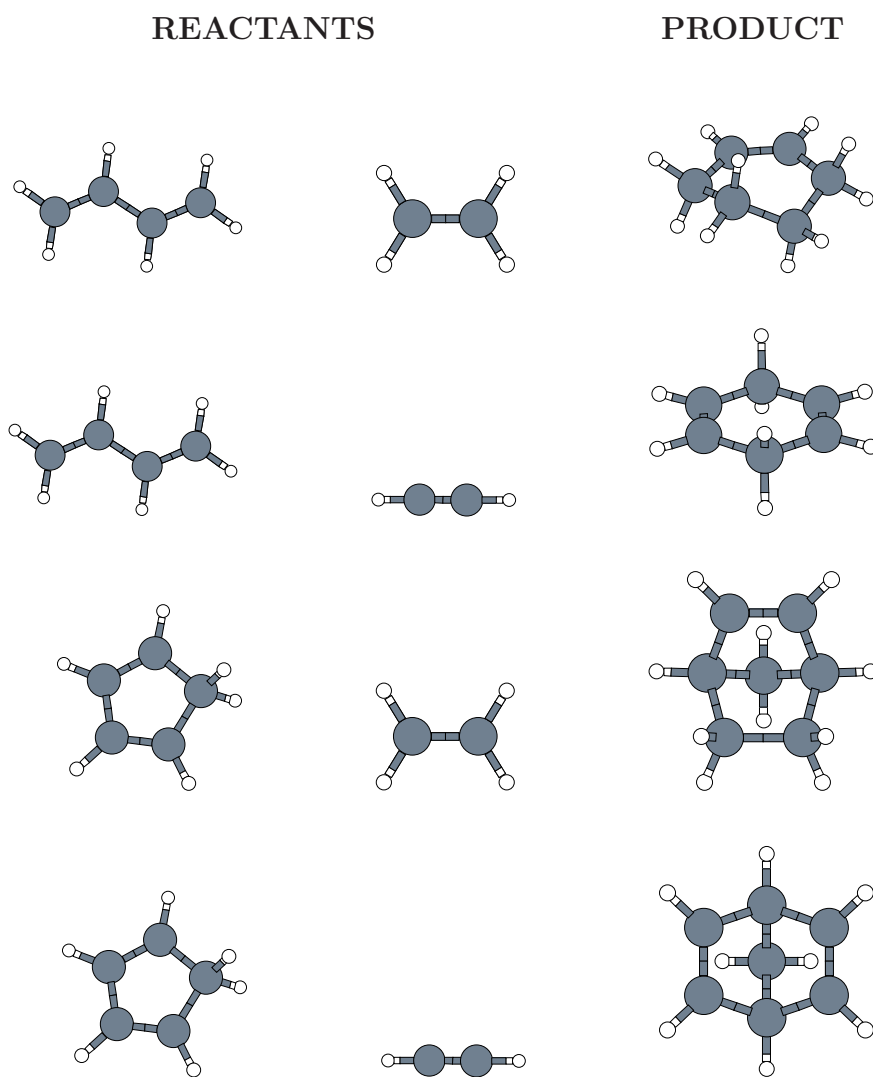Figure 1.

Figure 2.

28

(a)

(b)

Figure 3.

1
2
3
4
5
6
7
8
9
10
11
12
13
14
15
16
17
18
19
20
21
22
23
24
25
26
27
28
29
30
31
32
33
34
35
36
37
38
39
40
41
42
43
44
45
46
47
48
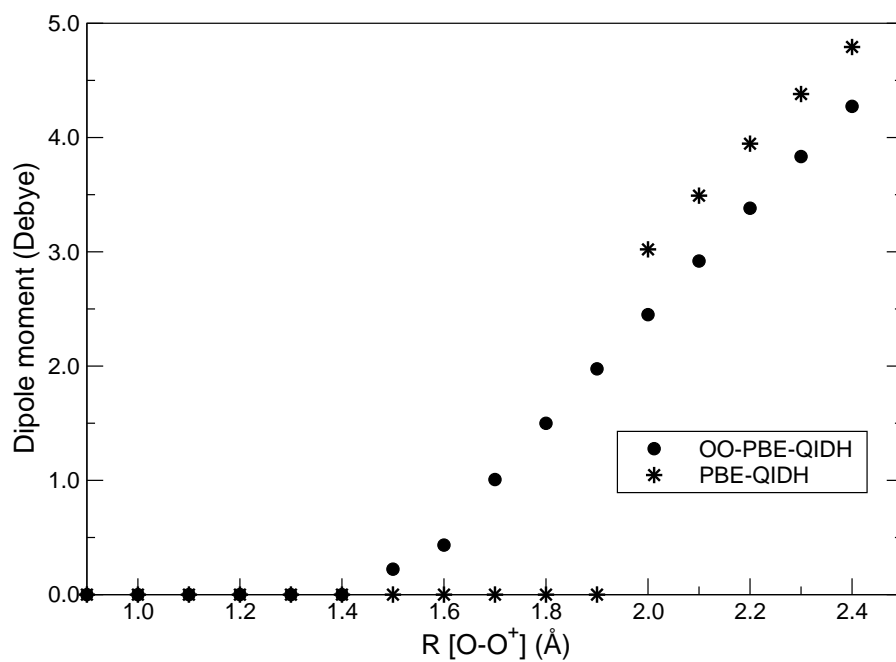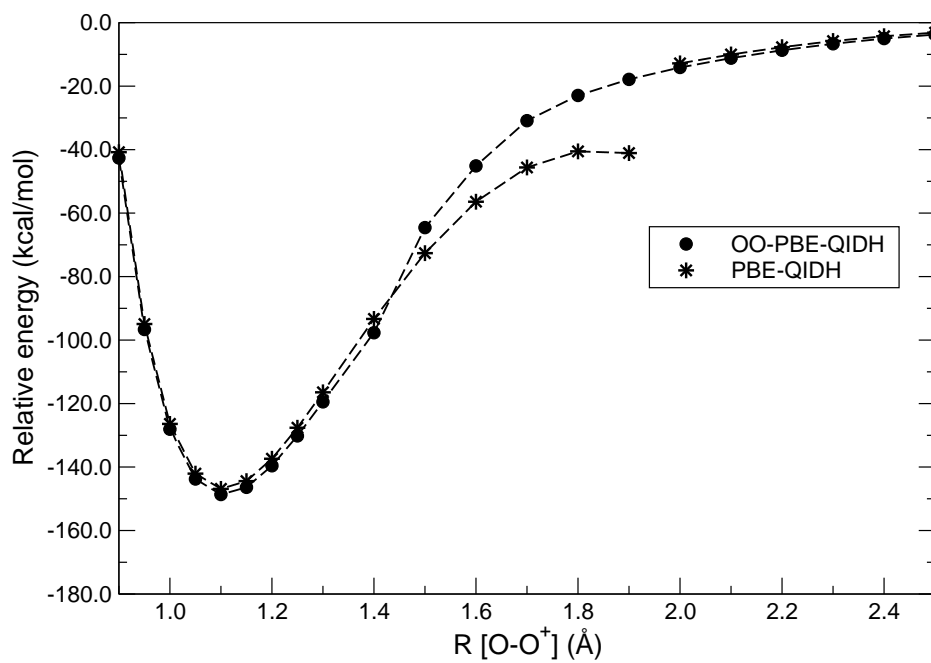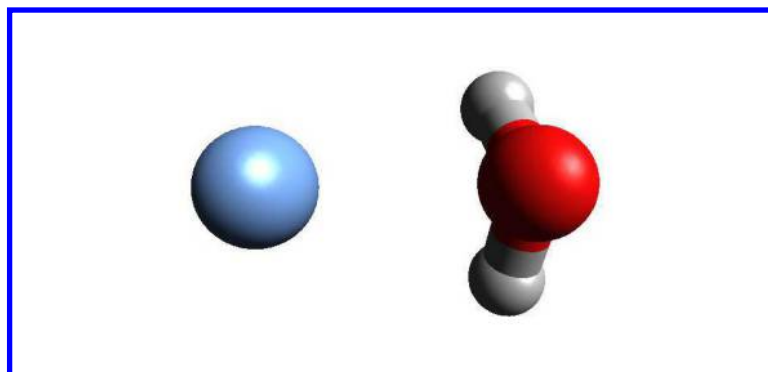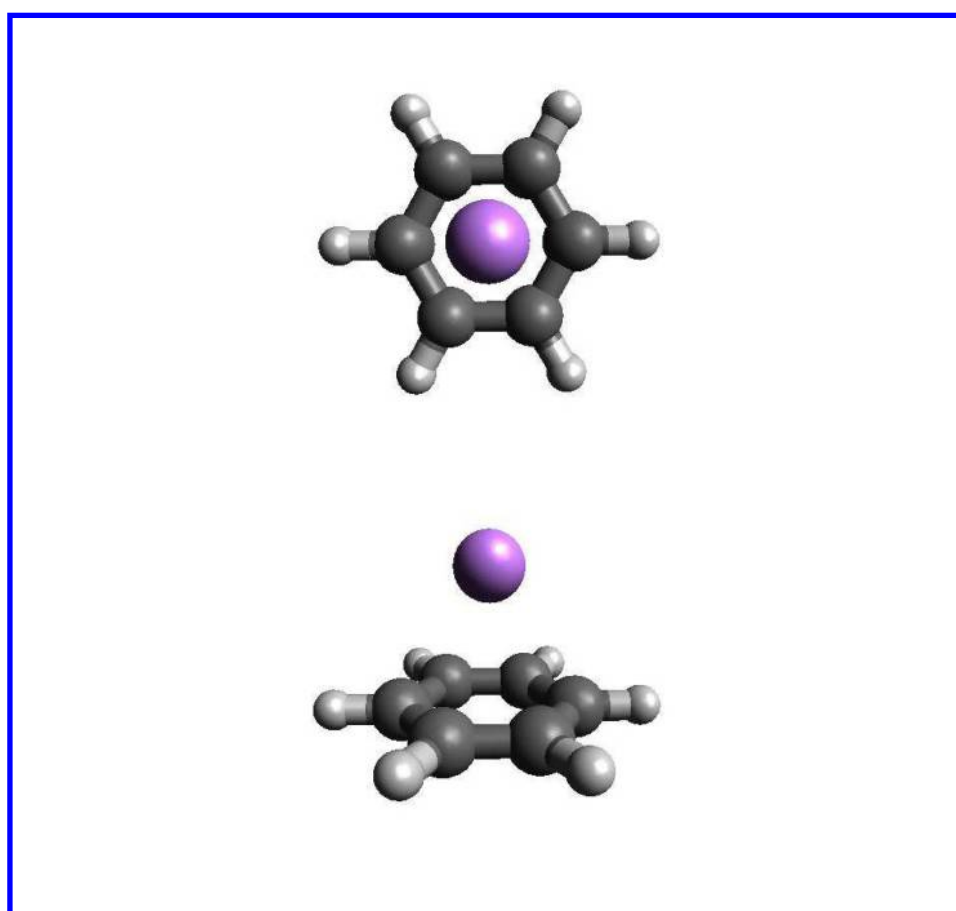49
50
51
52
53
54
55
56
57
58
59
60

Figure 4.

1
2
3
4
5
6
7
8
9
10
11
12
13
14
15
16
17
18
19
20
21
22
23
24
25
26
27
28
29
30
31
32
33
34
35
36
37
38
39
40
41
42
43
44
45
46
47
48
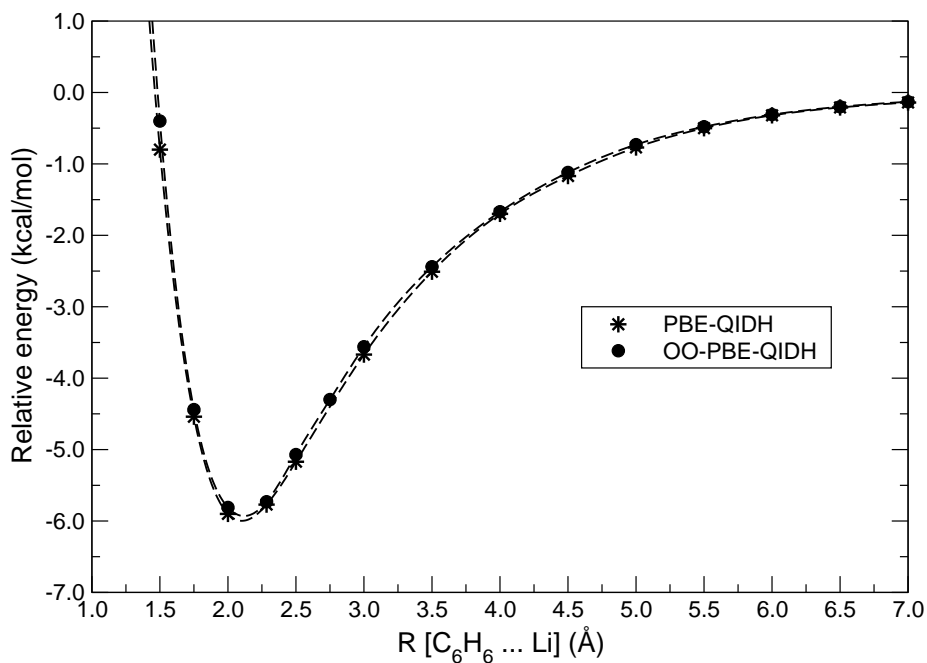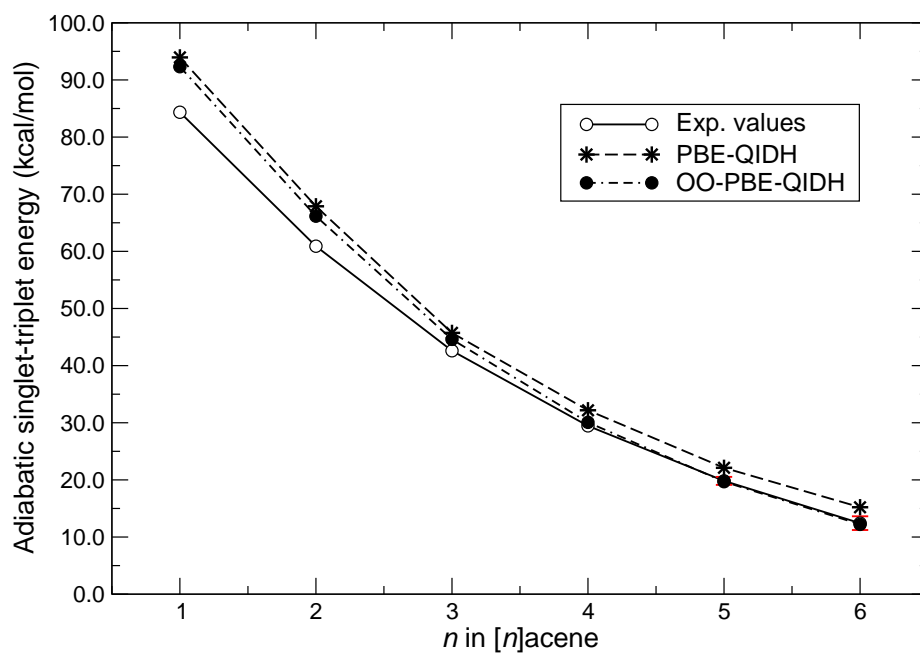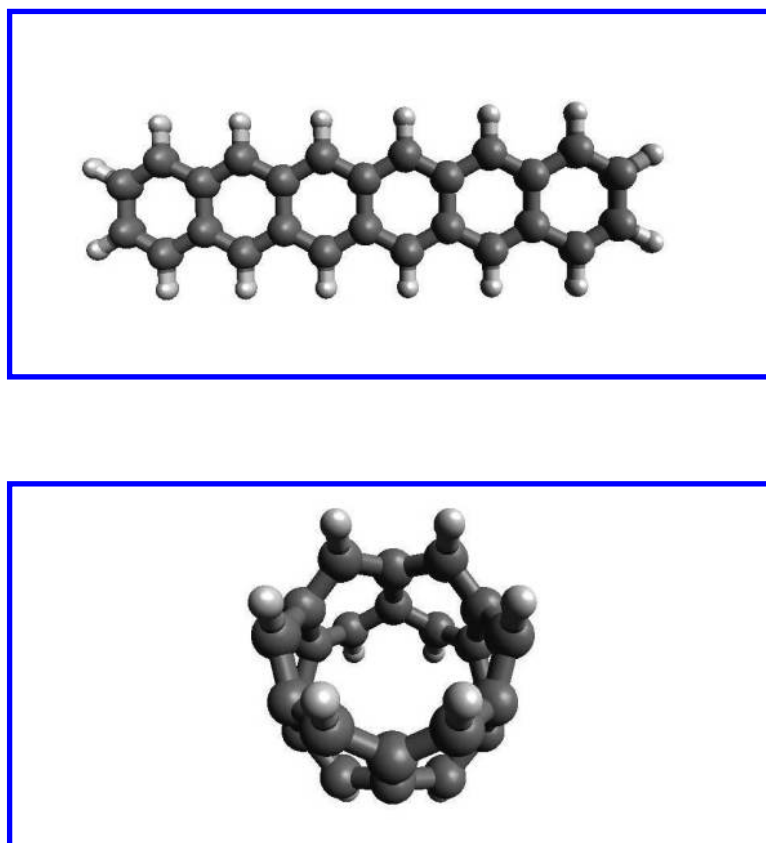49
50
51
52
53
54
55
56
57
58
59
60
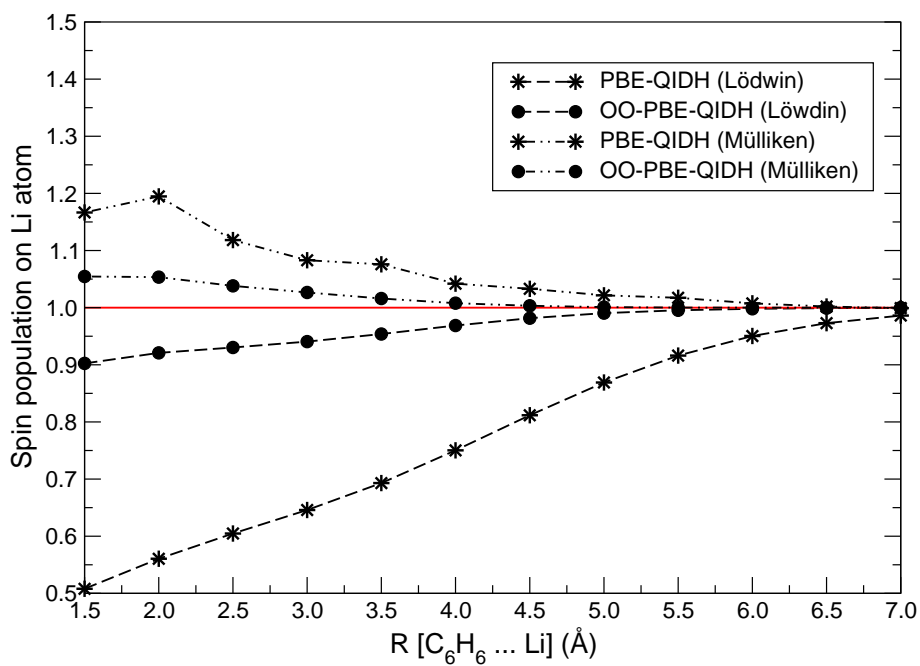
Figure 5.

Figure 6.

$$E_{xc}^{\mathrm{OO-PBE-QIDH}} = \underbrace{\lambda_x E_x^{\mathrm{EXX}}[\phi] + (1-\lambda_x)E_x[\rho] + (1-\lambda_c)E_c[\rho]}_{\mathrm{KS\ orbitals}} \underbrace{+\lambda_c E_c^{\mathrm{PT2}}[\phi,\phi']}_{\mathrm{Optimized\ MP2\ orbitals}}$$